

RESEARCH

Open Access



Estimating the cost of sea level rise

Magnus Hieronymus^{1*}, Jim Hedfors², Lisa Van Well², Gunnel Göransson³, Sebastian Bokhari Irminger² and Åke Magnusson²

Abstract

Sea level rise exacerbates flood risk for coastal communities globally. Multiple studies have shown that significant property values are already at risk this century, especially in high-emission scenarios. Thus, sea level rise poses major challenges that cannot be effectively addressed by many existing flood risk management methods. Some challenges include managing uncertainties, time dependence, and the interplay between mean sea level rise and extremes. Here, these components are integrated into a joint probabilistic framework, with the novelty of the approach being the direct connection of these factors to economic risk. The resulting framework provides a probabilistic assessment of flooding loss conditioned on user-defined emission scenario probabilities. The framework fits well as a tool for risk assessment, uncertainty quantification, and decision support. A major takeaway is that the risk increase accelerates with warming. Another takeaway is that the objectivity of flood risk assessments decreases significantly with increasing assessment length, with flood risk becoming more dependent on mean sea level change. The framework requires only readily available data and an open source model, enabling better-informed risk assessments through improved data utilization. The framework is validated using data from Kalmar city, one of Sweden's oldest cities, located in the south and known for its rich cultural heritage.

Keywords Flood risk, Sea level extremes, Sea level rise, Simulations

1 Introduction

Sea level rise is arguably among the most problematic consequences of global warming. A primary concern encompasses flood risk management for built and planned infrastructure (Hauer et al., 2021; Vousdoukas et al., 2018, 2020). However, existing coastal flood risk management methods are in many ways inadequate to tackle the challenge accompanying rising sea levels. Two primary limitations are that most of these methods fail to account for the probabilistic nature of sea level changes or the fact that flood risk varies considerably with time (Hieronymus, 2022; McEvoy et al., 2021). Such static

methods cannot exploit available, time-dependent, and probabilistic sea level data, making them suboptimal and prone to misjudgments. Moreover, physical risk (high sea levels) is seldom comprehensively connected to economic risk (from flooding) in climate adaptation decision support documents, thereby complicating decision-making (Auffhammer, 2018; Dawson et al., 2018).

This study addresses the development of an integrated probabilistic framework that simultaneously manages uncertainties, time dependencies, and the interplay between mean sea level rise and extremes, followed by linking them to economic risk. This provides a comprehensive assessment of flood-related losses conditioned on user-assigned probabilities of emission scenarios. The framework is tested in the pilot case of Kalmar, a culturally and historically significant city of approximately 73,000 inhabitants on the southeast coast of Sweden.

From a natural science perspective, flood risk is often considered a two-component problem encompassing: Mean sea level rise which is primarily due to

*Correspondence:

Magnus Hieronymus
magnus.hieronymus@smhi.se

¹ Oceanographic Research Unit, Swedish Meteorological and Hydrological Institute, Norrköping 60176, Sweden

² Swedish Geotechnical Institute, Linköping 58193, Sweden

³ Environmental Unit, Swedish National Road and Transport Research Institute, Linköping 41755, Sweden

© The Author(s) 2026. **Open Access** This article is licensed under a Creative Commons Attribution 4.0 International License, which permits use, sharing, adaptation, distribution and reproduction in any medium or format, as long as you give appropriate credit to the original author(s) and the source, provide a link to the Creative Commons licence, and indicate if changes were made. The images or other third party material in this article are included in the article's Creative Commons licence, unless indicated otherwise in a credit line to the material. If material is not included in the article's Creative Commons licence and your intended use is not permitted by statutory regulation or exceeds the permitted use, you will need to obtain permission directly from the copyright holder. To view a copy of this licence, visit <http://creativecommons.org/licenses/by/4.0/>.

anthropogenic climate change (Edwards et al., 2021; Fox-Kemper et al., 2021; Frederikse et al., 2020), and sea level extremes. Sea level extremes can also be affected by climate change, e.g., changes in storm tracks and the large-scale atmospheric circulation; however, they are primarily caused by weather events. Mean sea level rise is currently occurring at a globally averaged rate (3–4 mm/year) depending on the period and is accelerating (Dangendorf et al., 2024; Fox-Kemper et al., 2021). Meanwhile, sea level extremes can reach amplitudes of several meters depending on the location; however, they generally have durations counted in hours rather than centuries or millennia, which are appropriate time scales for mean sea level change (Fox-Kemper et al., 2021; Golledge et al., 2015; Marcos et al., 2009).

Mean sea level change and, especially, sea level extremes vary considerably at regional and local scales (Almar et al., 2021; Melet et al., 2018; Wahl et al., 2017). Extreme sea level data for planning are typically presented as return period–return level plots that show the yearly probability of the sea level reaching a given height over the current mean sea level (Arns et al., 2017). For a fixed return period, the return level may differ by meters, even between geographically close locations, depending on their exposure to storm surges and waves, as well as their tidal ranges (Muis et al., 2019; Soomere, 2023). Essentially, this indicates that flood risk must be evaluated at regional or even local scales.

Spatial heterogeneities are also considerable in mean sea level change. Sea level change may even be negative relative to land in areas with large glacial isostatic adjustment, whereas areas of subsidence may experience much higher than average rises (Hieronymus & Kalén, 2020; Nicholls et al., 2021). Mean sea level projections—representing sea level as a function of time across different shared socioeconomic pathways (SSPs)—are mostly used for planning purposes (McEvoy et al., 2021; Tamura et al., 2019). These projections typically include uncertainty ranges or are fully probabilistic, providing a distribution of possible future mean sea levels for each time step. However, the SSPs governing future greenhouse gas and aerosol emissions, land use, and other climate forcings are not probabilistic; they have no generally accepted occurrence probability (Huard et al., 2022; Srikrishnan et al., 2022).

A common method for determining design heights for new coastal infrastructure, which is also used in Kalmar, involves selecting a future mean sea level, typically a high percentile from a high emission projection, and adding a return level for sea level extremes corresponding to a long return period (Arns et al., 2017; Hieronymus, 2022). An additional margin corresponding to other unknowns is also typically added. One issue with such design heights

is that although the existing flood risk may be assumed to be small if a high return level, high emission scenario, and remote date are selected, there is no way of determining how high it is or its changes over time. Essentially, the approach conceals the uncertainties involved. These shortcomings are essentially due to the probabilistic information in sea level projections and return levels not being used to determine the design height.

A solution to this problem has been recently proposed and refined (Hieronymus, 2022, 2023; Hieronymus & Kalén, 2022). This solution consists of an annual maximum sea level simulator that integrates mean sea level projections and extreme sea level distributions into a joint probabilistic framework, in which flooding probabilities are estimated per planning period. Specifically, one simulates sea levels over a user-defined planning period (e.g., the expected service life of a structure) over many iterations. From this set of modeled planning periods, exceedance probabilities are determined relative to the current mean sea level. Moreover, emission scenarios are rendered probabilistic through occurrence-probability assignment. Thus, the flooding probabilities within the planning period are conditioned on user-defined emission scenario probabilities; consequently, uncertainty quantifications can be readily performed by varying these inputs. This eliminates the need for the arbitrary selection of mean and extreme sea levels; instead, planning can be based directly on the calculated flooding probabilities within the planning period. Essentially, they can be tailored to suit a planner's beliefs about the likelihood of different scenarios and his/her risk tolerance.

To estimate economic consequences, we construct a cost curve using the value of the building stock situated below given heights above the current mean sea level. In our example, the most accessible and comprehensive data for property value is the taxation value, which represents 75% of the estimated market value of properties from two years before the taxation assessment. Notably, while values in an urban environment, such as Kalmar, can be estimated relatively accurately using the value of the building stock, this is not applicable in all contexts. However, the described method works independently of how these values are assessed. The model simply requires a function that connects heights above sea level to an assessed value.

This same flexibility extends to the selection of sea level data. In the examples provided, we utilize mean sea level projections from the sixth assessment report of the Intergovernmental Panel on Climate Change (IPCC AR6) (Fox-Kemper et al., 2021), and data on sea level extremes derived from a long tide gauge series. However, any similarly structured data can be used, even personal prior probabilities. Thus, risk assessments using this tool can

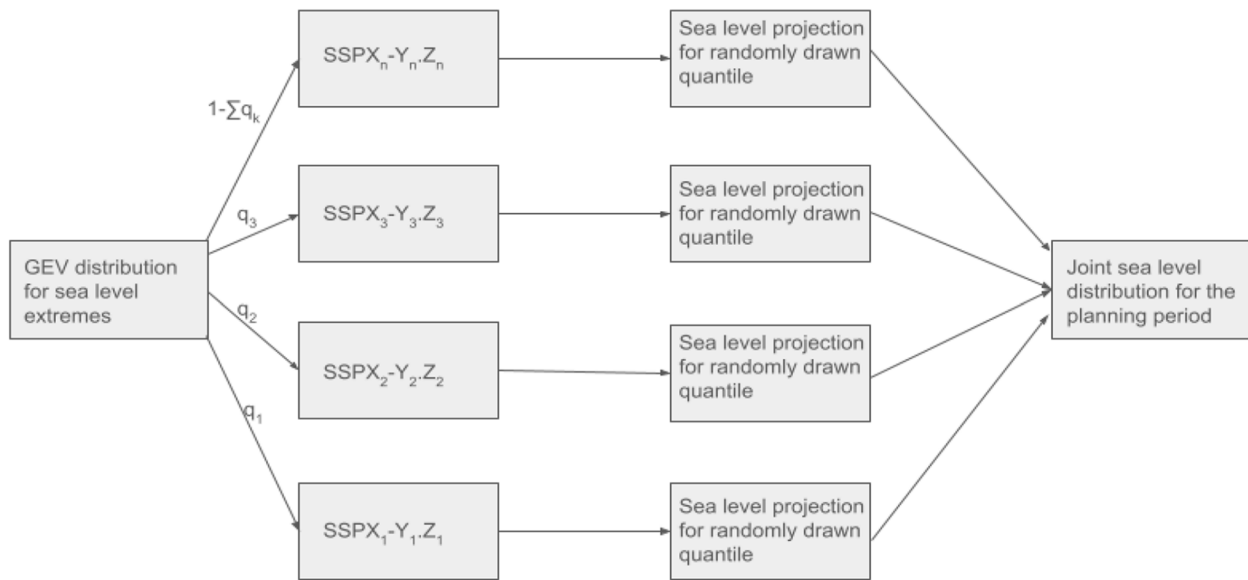


Fig. 1 Schematic of the sea level simulator. In the first box, a set of random annual maxima is drawn for the planning period. The second set of boxes determines the shared socioeconomic pathway (SSP) and mean sea level projection for the planning period. The third set of boxes selects a random quantile of the mean sea level projection for the given SSP. The fourth box adds the extremes to the mean sea level projection and calculates the joint planning period exceedance probabilities. The different q_k determine the probability of obtaining the corresponding SSP–radiative forcing combination. The summation over q_k goes over $k \in [1, n-1]$. Each planning period is modeled 10^7 times

be generated for any location, although the quality of the assessment will depend on the availability of local data.

2 Materials and methods

2.1 Sea level simulations

Our joint sea level projections are generated using the sea level simulator v1.0 (Hieronymus, 2022, 2023; Hieronymus & Kalén, 2022), which is open-source and available through https://github.com/m-hieronymus/the_sea_level_simulator. For a detailed model description, an interested reader is mainly referred to Hieronymus (2023); the description provided here is more condensed, focusing on the essential background for understanding the simulation process.

The simulator utilizes mean sea level projections—in our case, from IPCC AR6 (Fox-Kemper et al., 2021), together with a generalized extreme value (GEV) distribution for extreme sea levels derived from tide gauge data. The GEV parameters are estimated based on a block maxima approach with a one-year block length, and the maximum likelihood method is applied. The raw tide gauge data are also linearly detrended to eliminate land uplift and mean sea level changes. The IPCC AR6 mean sea level projections are corrected with a more accurate post-glacial land uplift estimate (Vestøl et al., 2019). The tide gauge data are sourced from the Kungsholmsfort station south of Kalmar, which provides a near continuous hourly record dating back to 1886. The GEV parameters

are assumed to be stationary and independent of the SSPs, following a recent study (Hieronymus & Hieronymus, 2023).

Figure 1 shows a schematic of the operational framework of the sea level simulator. As shown in the figure, every planning period is simulated 10^7 times. For each modeled period, a mean sea level projection, a mean sea level projection quantile, and a set of annual maxima are drawn randomly from their respective distributions. The annual maxima are relative to the current mean sea level and are sampled from the tide gauge-based GEV distribution using the ‘gevrnd’ function in MATLAB. We denote these values as $E(t, p)$, where t represents the different years, and p denotes the planning period index. The mean sea level projection for each planning period is sampled randomly from $U(0, 1)$ and mapped to the different projections using the user-prescribed q_k values that provide the probability of realizing each projection. From the selected projection, a quantile is drawn randomly from $U(0, 1)$ and used for the entire projection planning period. Specifically, if the SSP draw yields SSP1-2.6 in planning period 10 of 10^7 , and the quantile draw yields 0.93, the mean sea level of the entire tenth planning period follows that SSP and quantile. This ensures physically consistent, autocorrelated mean sea level projections across all planning periods. In practice, mean sea level projections are available for every tenth year, with the mean sea level for years in between being determined

through linear interpolation. The mean sea level trajectories for the different planning periods are denoted $MSL(t, p)$. The final step consists of computing the sum, $E(t, p) + MSL(t, p)$, which we denote as the joint sea level. We extract the maxima from the time series of the joint and mean sea levels within each planning period and compute the exceedance probabilities.

Notably, the probabilities computed by this sea level simulator are planning period ones, not yearly probabilities like those typically used in coastal risk assessments and coastal spatial planning. For a given sea level, h , the planning period probability $P(h)$ is the probability that the maximum joint or mean sea level observed at any time during the planning period exceeds h . This is an important difference; yearly probabilities fluctuate when the mean sea level changes, and even modest changes in mean sea levels can cause significant changes in return periods (Hieronymus & Kalén, 2020; Oppenheimer et al., 2019). Conversely, the planning period probabilities are constant throughout, thus representing a more suitable metric for planning and risk assessment purposes.

2.2 Cost curve

The cost curve is computed from elevation data and developed through geographic information systems (GIS) overlay analysis. This method integrates information on the specific sea level rise required to flood different land areas with information on the location and use of building stock. For each building, a specific elevation is identified at which the structure becomes susceptible to coastal flooding. This sea level is called the threshold level of the building. The threshold levels of all buildings

are calculated and plotted in a cumulative graph, offering the user the choice of selecting a sea level and identifying the number of flood-susceptible buildings (or total taxation value) within an area.

The grid providing information on threshold levels exhibits a 1×1 m spatial resolution and a vertical accuracy of 0.05–0.1 m. For each square meter within Kalmar city, we have determined the specific sea level threshold required to induce flooding. A polygon layer representing the building distribution has been placed on this grid. The lowest grid value that affects any part of the polygon, that is, the lowest sea level where any part of the building risks flooding, is set as the threshold for the entire building polygon. This binary description, whereby a building is entirely flooded or unaffected, represents a simplification. For buildings in areas with large ground-level changes, e.g., semidetached houses, the interpretation of the results becomes ambiguous. Based on the relatively synoptic nature of this investigation, the method, which produces conservative results, is judged to be satisfactory. Building elevation and geolocation data are provided by the Swedish Mapping, Cadastral, and Land Registration Authority. The GIS analysis is performed by integrating a feature manipulation engine and SCALable GeOgraphic algorithms. Figure 2 outlines the geographic scope of the Kalmar study area.

To ensure an accurate representation of areas that can be flooded, it is important to open flow paths in the elevation model where culverts or similar structures allow water to pass under elevation ridges, such as roads or railways. These culverts are included through hydrological corrections based on the Hydrography Dataset from

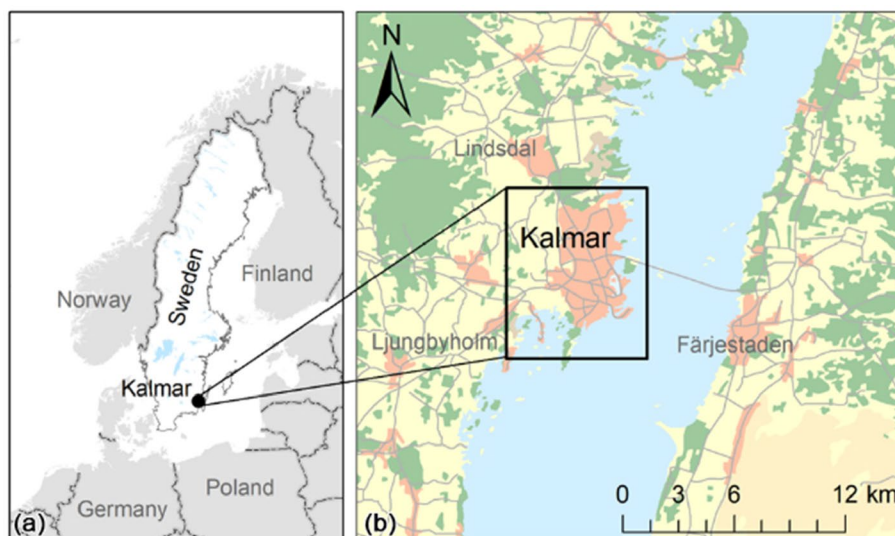


Fig. 2 Location of Kalmar city (a) and a magnified version with the geodata domain outlined by a black rectangle (b). Source: Lantmäteriet and SGI 2024

the Swedish Mapping, Cadastral, and Land Registration Authority, as well as road data and railway network from the Swedish Transport Administration.

The assessed monetary value of each residential property is linked to its corresponding threshold level through lookup tables of taxation values, linked via unique keys and integrated through GIS join-processing. Specifically, it will ignore any value related to roads, railroads, power grids, and other support facilities to only represent housing values. Additionally, no value change is observed over time. Such trends can, in principle, be incorporated into the simulator framework, although they are, like trends in sea level extremes, currently not considered.

Despite these caveats, our local cost and sea level curves provide a considerably more comprehensive coupling between economic and physical risks than is typically observed in similar assessments (Diaz & Moore, 2017). However, it must be noted that our study focuses on a much smaller geographical scale. Unfortunately, high spatial resolution is required to address considerable spatial heterogeneities in the joint sea level and cost curves.

2.3 Data integration

Figure 3 shows the planning period probability for joint sea levels across different SSPs, i.e., the synergistic effect of mean sea level change and extremes for Kalmar city, southern Sweden. In total, the 2020–2150 planning period was simulated 10^7 times per SSP. The red curve shows the cumulative taxation value of properties between the current mean sea level and that indicated on the x-axis.

An interesting aspect of the taxation value–sea level curve is the fact that it may contain thresholds. Specifically, there may be points on the curve where even a very small sea level rise can significantly increase taxation values under water. Such a threshold is visible at a sea level of ~5.5 m (Fig. 3). Here, the taxation value increases rapidly from approximately 18 to 21 BSEK, indicating significant value losses within very minor sea level changes. Identifying such threshold points can greatly aid planners in assessing time windows, scenarios, and probabilities leading to major changes, i.e., probable substantial value losses.

The 5.5 m threshold marks a shift from the susceptibility of single housing to sea level rise to that of more

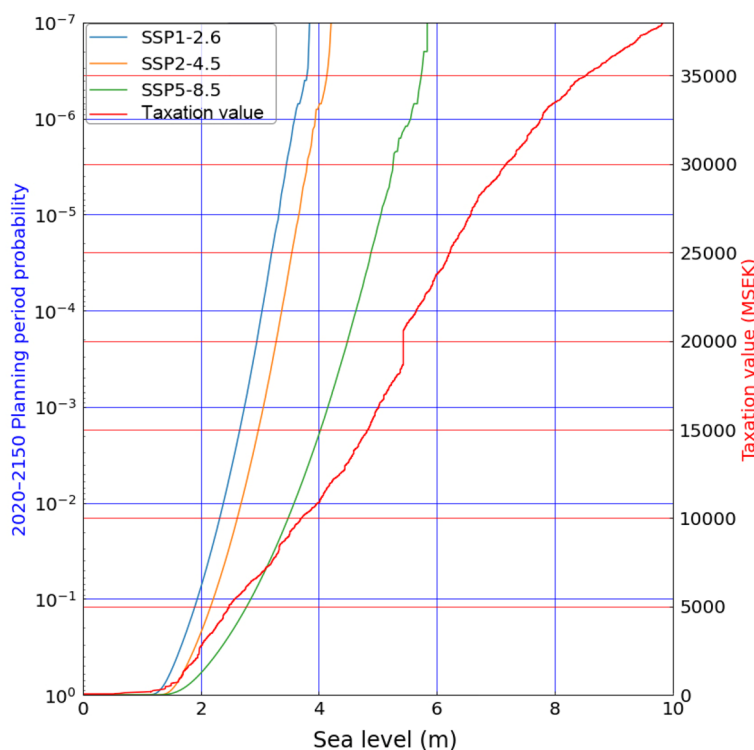


Fig. 3 Planning period probability and taxation value as a function of height above the current mean sea level. Red curve shows the cumulative taxation value of the properties situated below the sea level, shown on the x-axis. The blue, orange, and green curves show the planning period probability that the joint sea level will attain the sea level shown on the x-axis across the SSP1-2.6, SSP2-4.5, and SSP5-8.5 mean sea level projections, respectively. In total, the planning period was modeled 10^7 times per simulation. The calculations are performed using data from the Swedish city of Kalmar; the current mean sea level is assumed to be 0 m. Taxation values are given in million Swedish krona (MSEK)

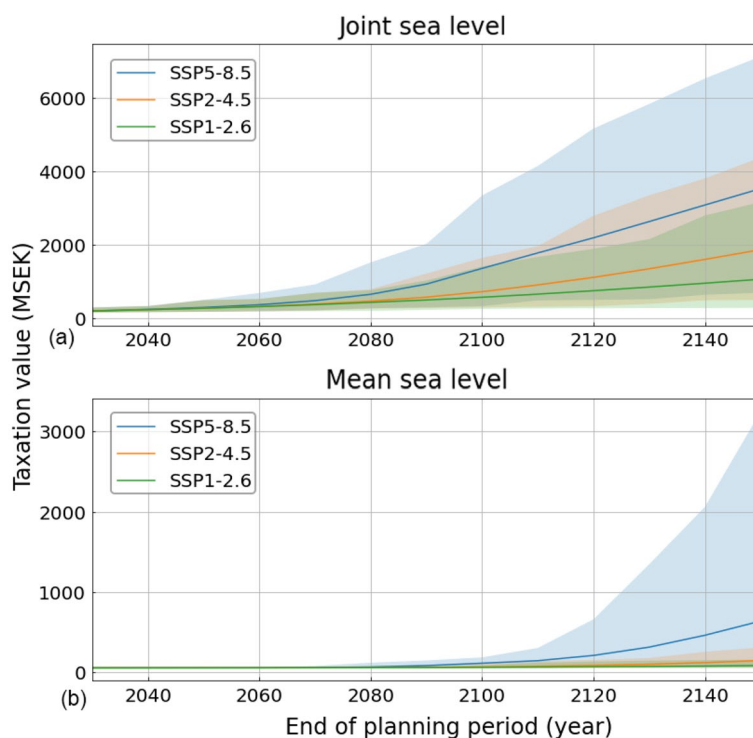


Fig. 5 Property values at risk across different SSPs. Median taxation values affected (solid lines) and their 0.05–0.95 quantile range (shading) as a function of the planning period length for joint sea level (a) and mean sea level (b). The x-axis shows the planning period end year, while the planning periods start in 2020 across all simulations. Three simulations are illustrated, where SSP5-8.5, SSP2-4.5, and SSP1-2.6 are each assigned an occurrence probability equal to one. The calculations are performed using data from Kalmar city. The taxation values are given in MSEK

in the planning period probability. Such a threshold is observed at approximately 5.5 m in Fig. 1 and illustrated geographically in Fig. 4.

A major uncertainty in any loss projection is the unknown occurrence likelihood of the different SSPs. However, current pledges and recent economic modeling, factoring in fossil fuel availability, provide some guidance at least. Broadly speaking, extremely low and high emission SSPs appear very unlikely under current policies,

especially when projected over long periods (Hausfather & Peters, 2020; Huard et al., 2022; Srikrishnan et al., 2022). To produce a less constrained projection that allows a larger variety of possible futures, we introduce a ‘mixed scenario’, where multiple SSPs are assigned a nonzero occurrence probability. The highest probability is assigned to SSP2-4.5, the scenario most compatible with current policies (Hausfather & Peters, 2020; Huard et al., 2022). We designate this the ‘mixed case.’ The scenario probabilities explored for the

Table 1 Probabilities, probability ranges, and estimated warming across the different mean sea level projections adopted in our ‘mixed case’ scenario

| Mean sea level distribution | Probability | Probability range | Estimated warming/°C (2081–2100 relative to 1850–1900) |
|-----------------------------|-------------|-------------------|--|
| SSP1-1.9 | 0.050 | [0, 0.050] | 1.4 |
| SSP1-2.6 | 0.155 | [0.050, 0.205] | 1.8 |
| SSP1-2.6 (low confidence) | 0.010 | [0.205, 0.215] | 1.8 |
| SSP2-4.5 | 0.500 | [0.215, 0.715] | 2.7 |
| SSP3-7.0 | 0.220 | [0.715, 0.935] | 3.6 |
| SSP5-8.5 | 0.064 | [0.935, 0.999] | 4.4 |
| SSP5-8.5 (low confidence) | 0.001 | [0.999, 1.000] | 4.4 |

The probability ranges show the range of randomly sampled scenario quantiles that correspond to each projection. The estimated warming is adopted from IPCC AR6. The low confidence projections utilize the same radiative forcing scenarios as their counterparts

mixed case are presented in Table 1. In the ‘mixed case’, as well as subsequent analyses, we also adopt the IPCC AR6 low confidence projections, where the ice sheet contributions to sea level rise are derived from some of the highest estimates reported in published scientific literature (Bamber et al., 2019; DeConto et al., 2021). The probabilities for the ‘mixed case’ are inspired by the scenario-specific probability estimates of Huard et al. (2022) for the later parts of the twenty-first century. These benchmarks are integrated with our assessments and further constrained to ensure that all scenarios maintain a nonzero probability. These results are intended as a demonstration case rather than a ‘best practice’ recommendation. Specifically, they represent a plausible prior sampled from a much larger set. Moreover, as with any prior of this kind, the results are affected by the discretization. More precisely, this results from the discretization process, which constrains a continuous set of beliefs in future sea level sensitivities and emissions into a discrete set of seven distinct probability distributions.

Figure 6 shows the expected amount of taxation values affected across the different projections as a function of planning period length. The expected values significantly depend on the scenario, especially when considering the SSP5-8.5 low confidence scenario that features a multimeter sea level rise from a rapidly collapsing Antarctic ice sheet. Notably, if we adopt SSP2-4.5 as the most plausible future, then much more is achieved by avoiding the highest scenarios than by reaching the very lowest. This is an asymmetry that is underappreciated and can be better accounted for in mitigation-goal setting. The Paris Agreement’s goal of limiting global warming to well below 2 °C, and preferably 1.5 °C, relative to pre-industrial levels, does not fully emphasize the fact that all warming scenarios increase risk, although the risk increase rate per degree of warming accelerates with warming. In essence, the 0.5 °C between 1.5 °C and 2 °C of warming is less risky than that between 2 °C and 2.5 °C, etc. Table 1 presents the estimated global mean temperature changes across the different emission scenarios.

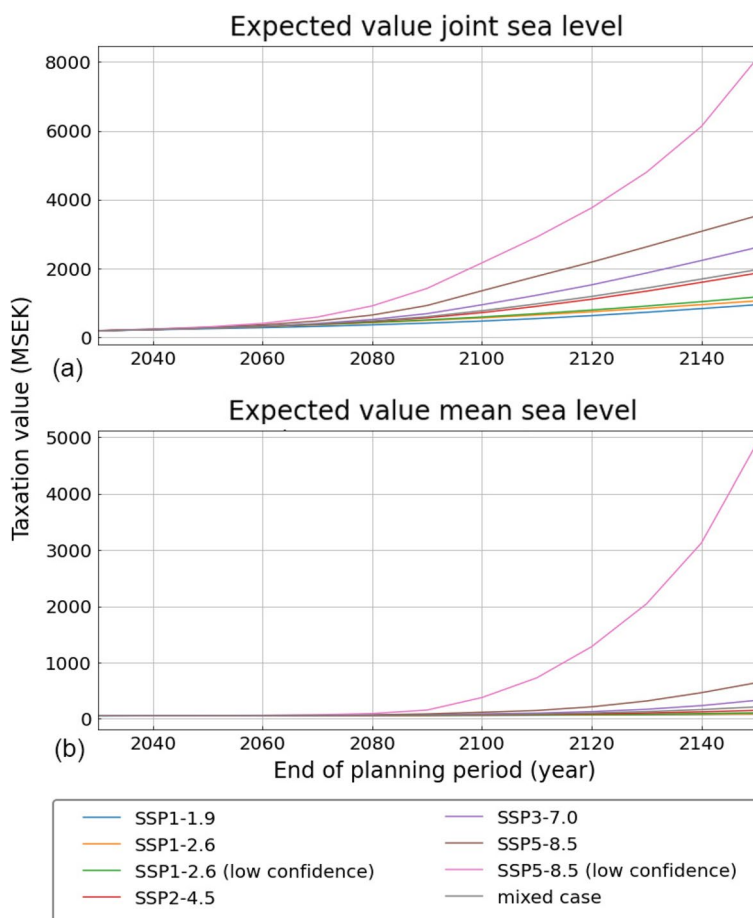


Fig. 6 Expected value of affected taxation values as a function of the planning period length across all scenarios for joint (a) and mean sea level (b). All planning periods start in 2020; their end date is given on the x-axis

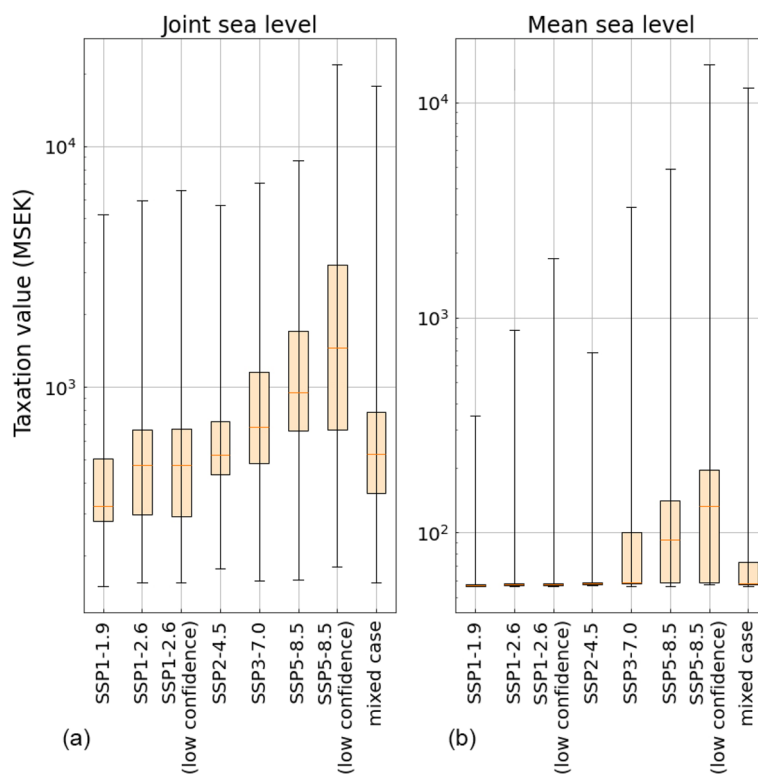


Fig. 7 Boxplot of the affected taxation values owing to joint sea level (a) and mean sea level (b) change over the 2020–2100 planning period for the different projections. The red lines show the median, and the boxes show the interquartile range. The whiskers show the highest and lowest values encountered during any simulated planning period for the respective scenarios. The whiskers essentially show the planning period probability range between 1 and 10^{-7} . The adopted data are for the Swedish city of Kalmar

This asymmetry is even more accentuated when considering ranges of possible outcomes across the different scenarios (Fig. 7); those ranges are displayed for the 2020–2100 planning period. The plot whiskers indicate the highest and lowest affected taxation values encountered during any of the 10^7 modeled planning periods for each projection. The much more right-skewed projection for the higher SSPs, especially the SSP5-8.5 low confidence projection, yielded some extreme values. There is approximately an order of magnitude difference between the highest affected taxation values encountered during the 2020–2100 planning period in the SSP5-8.5 low confidence and SSP1-1.9 projections when estimated based on the joint sea level. This divergence expands to almost two orders when estimated based on the mean sea level change. Notably, the ‘mixed case’ projection features a much higher maximum affected taxation value than even SSP5-8.5, despite the median and interquartile range being much lower in this projection. This is attributed to the inclusion of the SSP5-8.5 low confidence projection in the ‘mixed case’. Although assigned a low probability, all the extreme planning periods modeled in the ‘mixed

case’ occurred when the mean sea level projection follows the SSP5-8.5 low confidence projection.

A challenge in inferring economic losses from our simulations is that it may be overly pessimistic to equate, at least a low probability, a joint sea level to a full loss of property value. However, a property situated at the mean sea level will almost certainly have lost almost all its value. Thus, the difference between the property values affected by mean and joint sea levels can indicate the uncertainty in the projected losses, as illustrated in Fig. 8. The top panel in this figure shows the difference between the top and bottom panels of Fig. 6, and the bottom panel shows this difference normalized by the expected affected taxation values due to mean sea level rise. The top panel shows that the loss uncertainty is considerable and increasing with time. The bottom panel shows how large this uncertainty range is compared with the almost certain loss occurring when a property is situated at the mean sea level. The normalized curves peak before 2150 across all projections except for SSP1-1.9 and SSP1-2.6, indicating that the proportion of the affected taxation values due to extreme sea levels becomes less dominant

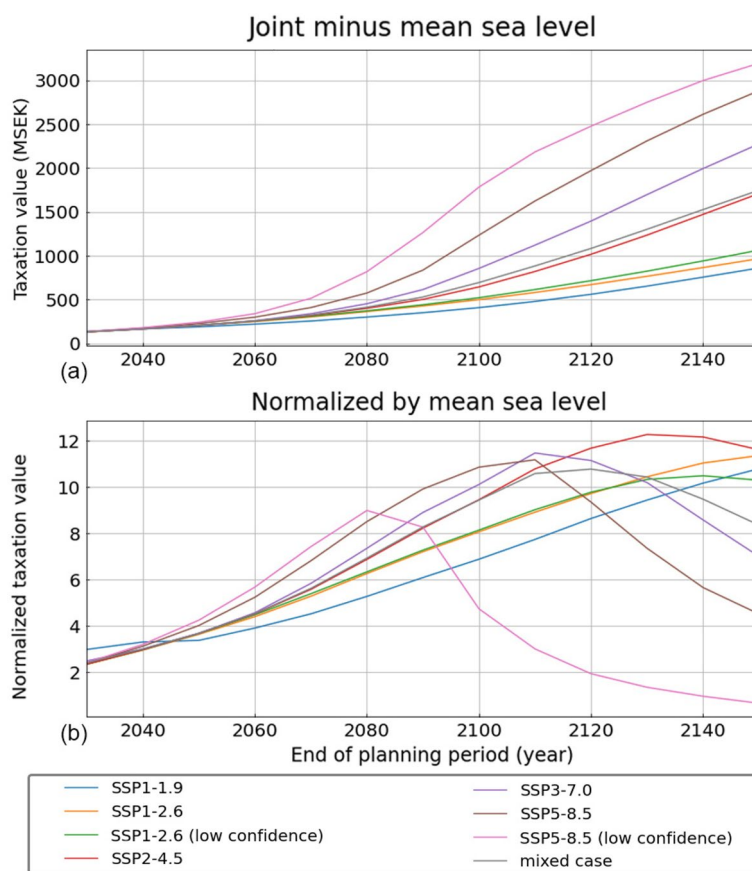


Fig. 8 Difference in the expected taxation values affected by joint (a) and mean (b) sea levels as a function of the planning period. The (a) panel shows the expected taxation values affected by the joint minus the mean sea levels. The (b) panel shows a normalized version, i.e., the expected taxation values affected by the joint minus the mean sea levels divided by the expected taxation values affected caused by the mean sea level

as the mean sea level rises and more properties become permanently inundated.

In short planning periods, flood risk is always dominated by sea level extremes, and in longer ones, it is dominated by a change in the mean sea level (Hieronymus, 2023; Hieronymus & Kalén, 2022). This follows directly from the yearly change in mean sea level being much smaller than the interannual variability in the annual maxima. The duration of the planning period required for the mean sea level component to dominate the risk assessment depends on local conditions. Figure 9 shows how the subjective probabilities that determine the mean sea level projection become more dominant in longer planning periods in the ‘mixed case’. The blue line shows the projection quantile (see Table 1) that corresponds to different property values affected by the joint sea level on average. The orange curve shows the projection quantile. In the 2020–2050 planning period, the affected property values are nearly independent of scenario (the probability is close to its average value of 0.5 for all taxation values affected). Conversely, the projection quantile is dominant

in determining the highest values. During longer projections, the affected taxation values strongly depend on both draws. Particularly, the taxation values affected start increasing rapidly under the upper part of the quantiles corresponding to the SSP2-4.5 projection on average. Notably, this does not necessarily indicate that the SSP2-4.5 scenario is responsible for this increase, as the figure shows the averaged quantile drawn. Some parts of the affected taxation values within this range may be caused by high and low quantiles of lower and higher SSP projections, respectively. For the 2020–2150 planning period, the upper two-thirds of the projected range of the affected taxation values occur only in the quantile range that corresponds to the SSP5-8.5 projections on average; the same is true of the upper half of the range in the 2020–2100 planning period.

4 Limitations and subjectivity

Well-informed decision-making is paramount to successful climate adaptation. However, in this context, with no perfect information to rely on, decisions must be taken

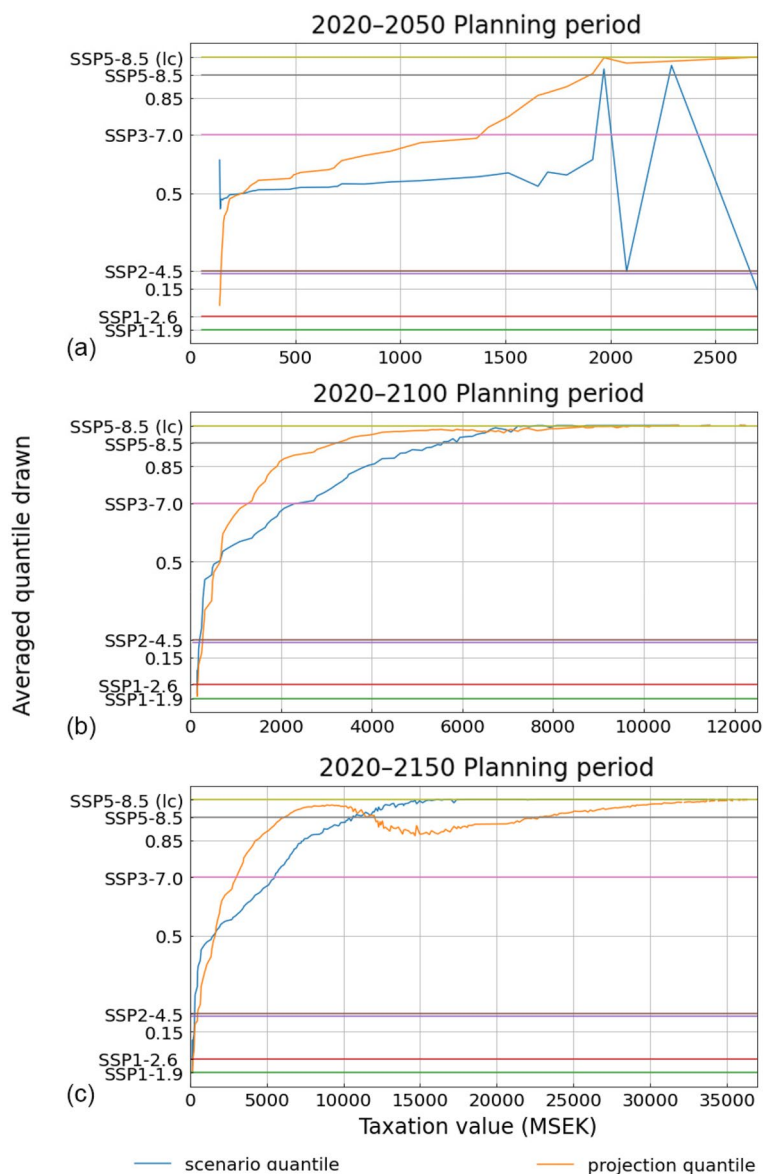


Fig. 9 Quantiles drawn and the corresponding property values at risk across different planning periods based on joint sea level for the ‘mixed case’. The blue lines show the scenario quantiles (i.e., the mean sea level projections drawn), and the orange line shows the quantile of the given projections that yield joint sea levels reaching different property values. The horizontal lines mark the quantiles for the different projections marked on the y-axis. Each projection occupies the quantile range between where it is marked and where the next projection is marked above it. The projection marking just below SSP2-4.5 shows Scenario SSP1-2.6 (low confidence). The ‘l’ after SSP5-8.5 denotes the ‘low confidence’ projection for the SSP5-8.5 scenario

under conditions of considerable uncertainty. The probabilities assigned to future emissions and mean sea levels are inherently subjective, with often expansive uncertainty ranges (Kopp et al., 2023; Slangen et al., 2023; van de Wal et al., 2022). Generally, probabilities are broadly categorized as objective or subjective. While objective probabilities correspond to frequencies of something observable, subjective probabilities correspond to degrees of belief in a given proposition. In this study,

the probabilities for sea level extremes are the only probabilities derived from the frequencies of an observable variable (historic tide gauge data). However, these observations are not recorded exactly within our area of interest. Since future emissions and mean sea levels are not observable, their respective probabilities are more accurately characterized as degrees of belief rather than as frequencies. Subjective probabilities are also called personal probabilities because, unlike objective probabilities,

they lack universality. In this sense, two perfectly reasonable persons may assign different probabilities to a given proposition, as there is no universal method for determining the correct ones.

Thus, risk assessments for future flooding are inherently personal or subjective, not due to methodological flaws, but because of the adopted data. Undoubtedly, this subjectivity can generate friction, as the risk assessed by a decision-maker may not correspond to that perceived by a coastal asset owner despite the former's conclusions directly impacting the latter's interest. While such friction is unavoidable, we believe that the tool presented in this study can alleviate it by explicitly clarifying how different assumptions and subjective choices affect the perceived flood risk, thus enabling a more informed discussion about coastal risk than what current decision support enables.

The planning period length is a critical factor determining the objectivity degree of a flood risk assessment. In short planning periods, the risk is dominated by the fairly objective extreme sea levels. However, Fig. 9 shows that the risk in long planning periods strongly depends on the subjective probabilities assigned to the different projected mean sea levels, signifying a strong control on the range of affected taxation values in long planning periods by the subjective choice of emission scenario probability.

An important question involves determining the flooding probability at which a property will begin to lose value. In short planning periods or in scenarios with limited mean sea level rise, one might assume value loss to be mostly caused by reparable damage and thus proportional to factors such as flood depth and flood duration. In longer planning periods, characterized by considerable mean sea level changes, this is unlikely to be a good assumption. In Sweden, as in many other countries, properties are only mortgaged if they are insured—insurance premiums will undoubtedly increase with the escalating flood risk. Moreover, the number of presumptive investors in coastal properties will almost certainly decrease when flood risk increases, owing to increasing insurance costs and an unwillingness to live in a house that is susceptible to non-negligible flood risks. Consequently, a value loss or an initiative to protect will likely be triggered before most properties are affected by flooding in a world with rapidly rising sea levels. Pinning down an exact relationship between flood risk and value loss appears almost impossible. Here, we conclude that unless protection is initiated, value loss will likely occur once the joint sea level reaches a probability quantile that prospective buyers consider an unacceptable risk. Furthermore, this value loss would, at least, be nearly finished by the time the mean sea level reaches the building's elevation.

Therefore, a planner must consider both joint and mean sea levels, as effective planning requires attention to multiple temporal scales. This challenge can be addressed by evaluating a range of potential climate adaptation measures and adopting a phased or dynamic decision-making approach that responds to emerging change signals. This will enhance flexibility by enabling successive pathways and adjustments over time (e.g., Grace & Thompson, 2020; Haasnoot et al., 2013).

As valuations are inherently subjective, using only property tax assessment values to estimate the economic consequences of flooding is admittedly a coarse simplification of the actual potential costs. Nevertheless, these values provide a valuable indicator of the water levels at which damage costs can be expected to increase sharply, regardless of their precise magnitude. In reality, costs depend on numerous factors; in the short term, these factors include the inundation duration, the floodwater depths, the coping capacity of the property or area to flooding, and the indirect costs associated with disruptions, such as reduced accessibility and mobility. In the long term, they entail properties that have become unsellable owing to the continuous rise in sea levels and coastal erosion. Additional costs relate to the temporary or long-term loss of natural and cultural values, recreational functions, and other benefits that cannot be readily quantified monetarily. Changes in property values over the planning period and the evolution of the building stock over the planning period also induce significant perturbations that are inherently challenging to estimate.

Another limitation is that the demonstrated framework only accounts for water levels relative to topography, failing to incorporate erosion processes. Consequently, erosion-induced failures, such as the collapse of bluffs, cliffs, or rocky shorelines, are neglected.

5 Framework versatility and scalability

While the examples described here are all based on Kalmar, a historic city with considerable cultural heritage, the same methods can be applied across other locations. Today, mean sea level projections and extreme sea level distributions are available with global coverage (Collings et al., 2024; Fox-Kemper et al., 2021). Moreover, the vast majority of countries maintain established property or land taxes alongside elevation maps on which detailed cost curve calculations can rely (Yamasaki et al., 2017); Zodrow, 2001). In areas where such data are unavailable or where values are not primarily concentrated in taxable assets, one may instead employ more subjectively assessed cost curves. Coarse resolution cost curves are already available with a global coverage (Huizinga et al., 2017), providing a viable baseline for risk assessments in data-sparse regions.

Sweden does not have a separate coastal zone planning system; instead, coastal planning is incorporated into the broader responsibility of the municipalities for physical environmental planning and the regulation of land and water use. Sweden's governance system is strongly decentralized, granting municipalities primary authority over spatial planning. Municipalities are also mandated to develop climate and vulnerability assessment frameworks for their territories. These assessments, as well as the municipal climate adaptation planning, provide the ideal framework for integrating materials, such as the findings of this study. This principle is equally applicable to countries that maintain dedicated coastal zone planning systems. While the framework does not necessarily provide a complete coastal planning tool, it illuminates the potential trade-offs in terms of valuations, which may be necessary. It can also integrate various types of valuation variables depending on the regional context. This could be a crucial starting point, especially in data-sparse regions.

For Kalmar municipality, the value of the framework lies in its ability to justify climate adaptation measures across different scenarios by illustrating the potential economic consequences for affected assets and activities. By visualizing these impacts, the framework facilitates the stimulation of political interest and engagement. It may also be valuable for stakeholders, such as real estate lenders and insurance companies, who rely on risk-informed decision-making.

Moreover, the demonstrated framework, particularly the cost curve, does not necessarily have to represent monetary costs. Multiple species will experience habitat loss as the sea rises. One example is mole skinks, a small reptile with five known subspecies found on a few islands off the Gulf Coast of Florida (Koen et al., 2024). Given a cost curve representing the area inhabited by mole skinks as a function of the height above the current mean sea level, one could replicate this analytical framework, although quantifying conservation values at risk instead of quantifying monetary loss. Given that sea level rise affects a vast array of natural and human systems, the potential applications of this methodology are extensive.

Expanding the spatial scale of the assessment is feasible; however, for a sufficiently large region, the large-scale cost has to be integrated through the summation of local cost estimates. Specifically, in the context of a global risk assessment of property values at risk, employing a universal joint sea level curve and cost curve will not provide an accurate estimate, as the exposure of infrastructure and other assets to mean and extreme sea levels varies considerably between locations.

6 Summary and conclusions

We have demonstrated that much more information is readily available in existing datasets than is typically utilized in sea level risk assessments, decision-making, and planning (Hieronymus, 2022; McEvoy et al., 2021). Focus is often concentrated on establishing a sufficient design height that preemptively avoids flood damage, at least in the near term. Current design height practice in Kalmar and more generally across Sweden, as outlined in the introduction, exemplifies this. Such a practice essentially conceals the associated uncertainties involved, shifting all the focus to a selected, but ultimately arbitrary level. The analyses presented in this paper not only draw attention to uncertainties but also help trace their causes. Based on a local cost curve, they can also directly connect flood risk to economic or other risks, depending on the nature of the cost curve. In essence, the framework makes risk a function of the planning period length and SSP probabilities instead of simply assuming a single mean sea level trajectory and a specific time, as is often the case (Hinkel et al., 2014; Vousdoukas et al., 2020). Taken together, these methods and data allow for more transparent and better-informed decision-making.

Sea level simulations, alongside cost curve calculations, can serve as decision support across a wide range of different contexts. Most directly, they form a cost-benefit analysis basis that informs decision-makers about the economic viability of different adaptation and mitigation measures. Adaptation and decision options can also be directly embedded in the simulator, aiding a dynamic view of climate adaptation, as well as enabling experimentation (Hieronymus, 2022).

Our case study reveals that the amount of taxation values at risk and their uncertainty increase rapidly with time. However, the risk is only weakly dependent on the subjective scenario probabilities for planning periods ending before 2050, while in longer planning periods, the more subjective uncertainties become dominant. This is particularly visible in the tails of the distributions of the taxation values at risk, where the highest values under the SSP5-8.5 low confidence projection are approximately an order-of-magnitude larger than those for the SSP1-1.9 projection in the 2020–2100 planning period for the joint sea level; these differences increased to nearly two orders for the mean sea level projection. In fact, Fig. 9 shows that a considerable part of the range of affected taxation values occurs only under the SSP5-8.5 projections in our simulations. However, it is important to note that having a large uncertainty span does not necessarily imply excessive expected taxation values at risk, as exemplified by the differences between the 'mixed scenario' and SSP5-8.5 (Figs. 6 and 7).

Another important takeaway illustrated in Figs. 6 and 7 is that risk increases with warming and per degree of warming. This essentially means that the risk increase from 2 °C to 3 °C of warming is larger than that from 1 °C to 2 °C. This is an important point that is often underappreciated in mitigation goal setting.

The cost-effective nature of sea level simulations and cost curve computations renders large-scale result integration feasible. Climate adaptation is becoming an integrated part of municipal spatial planning in large parts of the world; thus, the required competencies for conducting assessments such as this must be widespread. Moreover, as noted before, global datasets have already been established for cost curves, extreme sea level statistics, and mean sea level projections (Collings et al., 2024; Fox-Kemper et al., 2021; Huizinga et al., 2017). Although such coarse-resolution global datasets are not direct substitutes for detailed local analyses, they provide valuable first guesses in parts of the world lacking established detailed data.

Acknowledgements

We acknowledge Kalmar municipality and the COALA team for input and stimulating discussions around climate adaptation in the Kalmar area.

Authors' contributions

Magnus Hieronymus designed the study, performed most of the analysis and wrote the first draft. Jim Hedfors, Sebastian Bokhari Irminger and Åke Magnusson constructed the cost curve. Gunnel Göransson acquired funding. All authors contributed to the writing. All authors read and approved the final manuscript.

Funding

The research was funded by the FORMAS project: Klimatanpassning av kusten genom flexibel markanvändning (COALA) (No. 2021–02378).

Data availability

All data for mean sea level projections and observed sea level extremes are freely available through SMHI.se. The sea level simulator is available through https://github.com/m-hieronymus/the_sea_level_simulator.

Declarations

Ethics approval and consent to participate

Not applicable. This article does not contain any studies with human participants.

Competing interests

The authors declare that they have no competing interests.

Received: 13 January 2026 Revised: 6 May 2026 Accepted: 12 May 2026
Published online: 22 May 2026

References

- Almar, R., Ranasinghe, R., Bergsma, E. W. J., Diaz, H., Melet, A., Papa, F., et al. (2021). A global analysis of extreme coastal water levels with implications for potential coastal overtopping. *Nature Communications*, 12, 3775. <https://doi.org/10.1038/s41467-021-24008-9>
- Arns, A., Dangendorf, S., Jensen, J., Talke, S., Bender, J., & Pattiaratchi, C. (2017). Sea-level rise induced amplification of coastal protection design heights. *Scientific Reports*, 7, 40171. <https://doi.org/10.1038/srep40171>
- Auffhammer, M. (2018). Quantifying economic damages from climate change. *Journal of Economic Perspectives*, 32(4), 33–52. <http://acdc2007.free.fr/auffhammer18.pdf>
- Bamber, J. L., Oppenheimer, M., Kopp, R. E., & Cooke, R. M. (2019). Ice sheet contributions to future sea-level rise from structured expert judgment. *Proceedings of the National Academy of Sciences*, 116(23), 11195–11200. <https://doi.org/10.1073/pnas.1817205116>
- Collings, T. P., Quinn, N. D., Haigh, I. D., Green, J., Probyn, I., Wilkinson, H., et al. (2024). Global application of a regional frequency analysis to extreme sea levels. *Natural Hazards and Earth System Sciences*, 24, 2403–2423. <https://doi.org/10.5194/nhess-24-2403-2024>
- Dangendorf, S., Sun, Q., Wahl, T., Thompson, P., Mitrovica, J. X., & Hamlington, B. (2024). Probabilistic reconstruction of sea-level changes and their causes since 1900. *Earth System Science Data*, 16, 3471–3494. <https://doi.org/10.5194/essd-16-3471-2024>
- Dawson, D. A., Hunt, A., Shaw, J., & Gehrels, W. R. (2018). The economic value of climate information in adaptation decisions: Learning in the sea-level rise and coastal infrastructure context. *Ecological Economics*, 150, 1–10. <https://doi.org/10.1016/j.ecolecon.2018.03.027>
- DeConto, R. M., Pollard, D., Alley, R. B., Velicogna, I., Gasson, E., Gomez, N., et al. (2021). The Paris Climate Agreement and future sea-level rise from Antarctica. *Nature*, 593, 83–89. <https://doi.org/10.1038/s41586-021-03427-0>
- Diaz, D., & Moore, F. (2017). Quantifying the economic risks of climate change. *Nature Climate Change*, 7, 774–782. <https://doi.org/10.1038/nclimate3411>
- Edwards, T. L., Nowicki, S., Marzeion, B., Hock, R., Goelzer, H., Seroussi, H., et al. (2021). Projected land ice contributions to twenty-first-century sea level rise. *Nature*, 593, 74–82. <https://doi.org/10.1038/s41586-021-03302-y>
- Fox-Kemper, B., Hewitt, H.T., Xiao, C., Aðalgeirsdóttir, G., Drijfhout, S. S., Edwards, T. L. et al. (2021). 2021: Ocean, cryosphere and sea level change. In Masson-Delmotte, V., Zhai, P., Pirani, A., Connors, S. L., Péan, C., Berger, S. N. et al. (Eds.), *Climate Change 2021: The Physical Science Basis. Contribution of Working Group I to the Sixth Assessment Report of the Intergovernmental Panel on Climate Change* (pp. 1211–1362). Cambridge University Press, Cambridge. <https://imis.nioz.nl/imis.php?module=ref&refid=349351>
- Frederikse, T., Landerer, F., Caron, L., Adhikari, S., Parkes, D., Humphrey, V. W., et al. (2020). The causes of sea-level rise since 1900. *Nature*, 584, 393–397. <https://doi.org/10.1038/s41586-020-2591-3>
- Golledge, N., Kowalewski, D., Naish, T., Levy, R. H., Fogwill, C. J., & Gasson, E. G. W. (2015). The multi-millennial Antarctic commitment to future sea-level rise. *Nature*, 526, 421–425. <https://doi.org/10.1038/nature15706>
- Grace, B., & Thompson, C. (2020). All roads lead to retreat: Adapting to sea level rise using a trigger-based pathway. *Australian Planner*, 56(3), 182–190. <https://doi.org/10.1080/07293682.2020.1775665>
- Haasnoot, M., Kwakkel, J., Walker, W., & ter Maat, J. (2013). Dynamic adaptive policy pathways: A method for crafting robust decisions for a deeply uncertain world. *Global Environmental Change*, 23(2), 485–498. <https://doi.org/10.1016/j.gloenvcha.2012.12.006>
- Hauer, M. E., Hardy, D., Kulp, S. A., Mueller, V., Wrathall, D. J., & Clark, P. U. (2021). Assessing population exposure to coastal flooding due to sea level rise. *Nature Communications*, 12, 6900. <https://doi.org/10.1038/s41467-021-27260-1>
- Hausfather, Z., & Peters, G. P. (2020). Emissions—the ‘business as usual’ story is misleading. *Nature*, 577, 618–620. <https://doi.org/10.1038/d41586-020-00177-3>
- Hieronymus, M. (2022). A yearly maximum sea level simulator and its applications: A Stockholm case study. *Ambio*, 51, 1263–1274. <https://doi.org/10.1007/s13280-021-01661-4>
- Hieronymus, M. (2023). The sea level simulator v1.0: A model for integration of mean sea level change and sea level extremes into a joint probabilistic framework. *Geoscientific Model Development*, 16, 2343–2354. <https://doi.org/10.5194/gmd-16-2343-2023>
- Hieronymus, M., & Hieronymus, F. (2023). A novel machine learning based bias correction method and its application to sea level in an ensemble of downscaled climate projections. *Tellus*, 75(1), 129–144. <https://doi.org/10.16993/tellusa.3216>
- Hieronymus, M., & Kalén, O. (2020). Sea-level rise projections for Sweden based on the new IPCC special report: The ocean and cryosphere in a changing climate. *Ambio*, 49, 1587–1600. <https://doi.org/10.1007/s13280-019-01313-8>
- Hieronymus, M., & Kalén, O. (2022). Should Swedish sea level planners worry more about mean sea level rise or sea level extremes? *Ambio*, 51, 2325–2332. <https://doi.org/10.1007/s13280-022-01748-6>

- Hinkel, J., Lincke, D., Vafeidis, A. T., Perrette, M., Nicholls, R. J., Tol, R. S. J., et al. (2014). Coastal flood damage and adaptation costs under 21st century sea-level rise. *Proceedings of the National Academy of Sciences*, 111(9), 3292–3297. <https://doi.org/10.1073/pnas.1222469111>
- Huard, D., Fyke, J., Capellán-Pérez, I., Matthews, H. D., & Partanen, A. I. (2022). Estimating the likelihood of GHG concentration scenarios from probabilistic integrated assessment model simulations. *Earth's Future*, 10, e2022EF002715. <https://doi.org/10.1029/2022EF002715>
- Huizinga, J., de Moel, H., & Szewczyk, W. (2017). Global flood depth-damage functions: Methodology and the database with guidelines. JRC Publications Repository. <https://publications.jrc.ec.europa.eu/repository/handle/JRC105688>. Accessed 10 Oct 2025.
- Koen, E. L., Barichivich, W. J., & Walls, S. C. (2024). Vulnerability of endemic insular mole skinks to sea-level rise. *Conservation Science and Practice*, 6(9), e13208. <https://doi.org/10.1111/csp.2.13208>
- Kopp, R. E., Oppenheimer, M., O'Reilly, J. L., Drijfhout, S. S., Edwards, T. L., Fox-Kemper, B., et al. (2023). Communicating future sea-level rise uncertainty and ambiguity to assessment users. *Nature Climate Change*, 13, 648–660. <https://doi.org/10.1038/s41558-023-01691-8>
- Marcos, M., Tsimplis, M. N., & Shaw, A. G. P. (2009). Sea level extremes in southern Europe. *Journal of Geophysical Research*, 114, C01007. <https://doi.org/10.1029/2008JC004912>
- McEvoy, S., Haasnoot, M., & Biesbroek, R. (2021). How are European countries planning for sea level rise? *Ocean & Coastal Management*, 203, 105512. <https://doi.org/10.1016/j.ocecoaman.2020.105512>
- Melet, A., Meyssignac, B., Almar, R., & Le Cozannet, G. (2018). Under-estimated wave contribution to coastal sea-level rise. *Nature Climate Change*, 8, 234–239. <https://doi.org/10.1038/s41558-018-0088-y>
- Muis, S., Lin, N., Verlaan, M., Winsemius, H. C., Ward, P. J., & Aerts, J. C. (2019). Spatiotemporal patterns of extreme sea levels along the western North-Atlantic coasts. *Scientific Reports*, 9, 3391. <https://doi.org/10.1038/s41598-019-40157-w>
- Nicholls, R. J., Lincke, D., Hinkel, J., Brown, S., Vafeidis, A. T., Meyssignac, B., et al. (2021). A global analysis of subsidence, relative sea-level change and coastal flood exposure. *Nature Climate Change*, 11, 338–342. <https://doi.org/10.1038/s41558-021-00993-z>
- Oppenheimer, M., Glavovic, B. C., Hinkel, J., van de Wal, R., Magnan, A. K., Abd-Elgawad, A., et al. (2019). Sea level rise and implications for low-lying islands, coasts and communities. In Pörtner, H. O., Roberts, D. C., Masson-Delmotte, V., Zhai, P., Tignor, M., Poloczanska, E., et al. (Eds.), *IPCC Special Report on the Ocean and Cryosphere in a Changing Climate* (pp. 321–445). Cambridge University Press, Cambridge. <https://doi.org/10.1017/9781009157964.006>
- Slangen, A. B. A., Palmer, M. D., Camargo, C. M. L., Church, J. A., Edwards, T. L., Hermans, T. H. J., et al. (2023). The evolution of 21st century sea-level projections from IPCC AR5 to AR6 and beyond. *Cambridge Prisms: Coastal Futures*, 1, e7. <https://doi.org/10.1017/cft.2022.8>
- Soomere, T. (2023). Numerical simulations of wave climate in the Baltic Sea: A review. *Oceanologia*, 65(1), 117–140. <https://doi.org/10.1016/j.oceanol.2022.01.004>
- Srikrishnan, V., Guan, Y., Tol, R. S. J., & Keller, K. (2022). Probabilistic projections of baseline twenty-first century CO₂ emissions using a simple calibrated integrated assessment model. *Climatic Change*, 170, 37. <https://doi.org/10.1007/s10584-021-03279-7>
- Tamura, M., Kumano, N., Yotsukuri, M., & Yokoki, H. (2019). Global assessment of the effectiveness of adaptation in coastal areas based on RCP/SSP scenarios. *Climatic Change*, 152, 363–377. <https://doi.org/10.1007/s10584-018-2356-2>
- van de Wal, R. S. W., Nicholls, R. J., Behar, D., McInnes, K., Stammer, D., Lowe, J. A., et al. (2022). A high-end estimate of sea level rise for practitioners. *Earth's Future*, 10, e2022EF002751. <https://doi.org/10.1029/2022EF002751>
- Vestøl, O., Ågren, J., Steffen, H., Kierulf, H., & Tarasov, L. (2019). NKG2016LU: A new land uplift model for Fennoscandia and the Baltic Region. *Journal of Geodesy*, 93, 1759–1779. <https://doi.org/10.1007/s00190-019-01280-8>
- Vousdoukas, M. I., Mentaschi, L., Voukouvalas, E., Bianchi, A., Dottori, F., & Feyen, L. (2018). Climatic and socioeconomic controls of future coastal flood risk in Europe. *Nature Climate Change*, 8, 776–780. <https://doi.org/10.1038/s41558-018-0260-4>
- Vousdoukas, M. I., Mentaschi, L., Hinkel, J., Ward, P. J., Mongelli, I., Ciscar, J. C., et al. (2020). Economic motivation for raising coastal flood defenses in Europe. *Nature Communications*, 11, 2119. <https://doi.org/10.1038/s41467-020-15665-3>
- Wahl, T., Haigh, I., Nicholls, R., Arns, A., Dangendorf, S., Hinkel, S., et al. (2017). Understanding extreme sea levels for broad-scale coastal impact and adaptation analysis. *Nature Communications*, 8, 16075. <https://doi.org/10.1038/ncomms16075>
- Yamazaki, D., Ikeshima, D., Tawatari, R., Yamaguchi, T., O'Loughlin, F., Neal, J. C., et al. (2017). A high-accuracy map of global terrain elevations. *Geophysical Research Letters*, 44, 5844–5853. <https://doi.org/10.1002/2017GL072874>
- Zodrow, G. R. (2001). The property tax as a capital tax: A room with three views. *National Tax Journal*, 54(1), 139–156. <https://www.jstor.org/stable/41789538>

Publisher's Note

Springer Nature remains neutral with regard to jurisdictional claims in published maps and institutional affiliations.